PFC/JA-94-015

Power Balance and Scaling of the Radiated Power in the Divertor and Main Plasma of Alcator C-Mod

J.A. Goetz, B. Lipschultz, M.A. Graf,
C. Kurz, R. Nachtrieb, J.A. Snipes, J.L. Terry

Plasma Fusion Center
Massachusetts Institute of Technology
Cambridge, MA 02139

June 1994

Submitted to Journal of Nuclear Materials.

This work was supported by the U. S. Department of Energy Contract No. DE-AC02-78ET51013. Reproduction, translation, publication, use and disposal, in whole or in part by or for the United States government is permitted.

Power balance and scaling of the radiated power in the divertor and main plasma of Alcator C-Mod

J.A. Goetz, B. Lipschultz, M.A. Graf, C. Kurz, R. Nachtrieb, J.A. Snipes, and J.L. Terry

Plasma Fusion Center, Massachusetts Institute of Technology, Cambridge, MA 02139, USA

Measurements have been made of the radiation in the main plasma and divertor of Alcator C-Mod using bolometer arrays. It is found that the power radiated from the main plasma is $P_{rad,main} / P_{Ohmic} \sim 0.3 - 0.4$ over the range $0.2 \leq \overline{n}_e \leq 2.5 \times 10^{20}$ m^{-3}. There is significant radiated power coming from the divertor region; $P_{rad,divertor} / P_{Ohmic} \sim 0.4$. The radiated power in the main plasma and divertor scales linearly with density. When divertor detachment occurs, the power flow to the divertor plates in the region near the strike points is suddenly reduced, the fraction of the input power radiated from the main plasma and divertor increases, and the radiation in the divertor region is spatially rearranged.

1. Introduction

Energy can be removed from a tokamak plasma through radiation and charge exchange and is dissipated onto the surrounding walls and divertor surfaces. A considerable fraction of the input heating power of a tokamak plasma may be lost by impurity line radiation, mainly in the VUV to soft x-ray spectral range, and by neutral particles through charge exchange processes. This radiation, whether from the main plasma or the divertor, reduces the power incident on the divertor plates which is carried by conduction and convection of the plasma in the scrape-off layer. This is important for divertor operation in that it will ease the problem of removing the heat and cause less erosion of the divertor plates in future tokamaks and reactors. An overview of measurements of radiation from the initial operational period of the Alcator C-Mod tokamak [1] will be presented in this paper. Although capable of operating with a closed or open divertor, only results from operation with a closed shaped divertor will be discussed.

2. Bolometer systems

The bolometer systems installed in the tokamak are used to determine the local radiation emissivity and the total radiated power of the plasma (photons plus neutrals). The bolometers consist of blackened gold foil absorbers separated by an insulating foil from gold meander resistors [2]. The foils absorb neutrals and radiation from visible through x-ray energies. For main plasma measurements a toroidally-viewing array is used. This bolometer array has 24 chords that span the main plasma in

the midplane with two centimeter radial resolution. There are two poloidally-viewing bolometer arrays in the closed divertor region (see Figure 1), each consisting of four collimated detectors; one has horizontal views that encompass the inner strike point (chords B1 - B4), and one has horizontal views that encompass the outer strike point (chords B5 - B8). The third divertor array consists of sixteen XUV photodiodes that view the inner half of the closed divertor region (chords UV1 - UV16). These photodiodes are responsive to photons with energies from 50 eV to 10 keV but do not measure the energy from neutral particles.

3. Main plasma measurements

Chord brightness data obtained from the toroidally-viewing array of bolometers are Abel-inverted to obtain the radiation emissivity profile which is then volume-integrated to obtain the total radiated power from the main plasma. Data are selected from quiescent periods of discharges with constant current and density. A database has been constructed which includes data from discharges with plasma current in the range $0.4 \leq I_p \leq 1.0$ MA and line-averaged density in the range $0.2 \leq \overline{n}_e \leq 2.5 \times 10^{20}$ m^{-3}. The Ohmic input power is a function of the current and density and is in the range $0.4 \leq P_{Ohmic} \leq 1.4$ MW.

Typically the radiation emissivity profile is hollow with wings at a normalized radius of approximately 0.8. The major sources of error in this data are: uncertainties in the calibration constants of the bolometers of ± 20%, uncertainties in the electronics gains of ± 10%, and uncertainties in the radial location of the chords of ± 2%. Emissivity profiles of the intrinsic impurities, mainly carbon and molybdenum, obtained by modelling with

the MIST impurity transport code [3] correlate well with the radiation emissivity profiles obtained from the bolometer data.

In general it is found that the fraction of the input power radiated from the main plasma is $0.2 \leq P_{rad,main} / P_{Ohmic} \leq 0.4$ (see Figure 2) although there is a large variation in this fraction for low densities ($\overline{n}_e \leq 0.8 \times 10^{20}$ m^{-3}). This fraction does not change significantly as the density increases. However, the power radiated from the main plasma increases linearly with density when $\overline{n}_e \geq 0.8 \times 10^{20}$ m^{-3} (see Figure 2). This linear increase in the radiated power with density implies that the impurity concentration remains approximately constant over this range in density ($P_{rad} \sim n_e\, n_{imp}\, L_{imp}(T)$). The Z_{eff} of the plasma remains constant when $\overline{n}_e \geq 0.8 \times 10^{20}$ m^{-3}, which also implies that the impurity concentration is constant ($Z_{eff} \alpha n_{imp} / n_e$).

Spectroscopic measurements of the fractional abundances of impurities indicate that carbon, which originates from vessel and tile surfaces, is the dominant impurity with the oxygen concentration a factor of about three less than the carbon. The fractional abundance of carbon is $\leq 0.5\%$ and that of molybdenum, which is the first wall material, is approximately 0.02%. These abundances indicate that carbon and molybdenum contribute about 0.1 and 0.2 respectively to Z_{eff}. These values are in good agreement with the measured Z_{eff}.

Modelling using the MIST impurity transport code together with data obtained from a multi-layer-mirror based molybdenum diagnostic [4] and an absolutely calibrated grazing incidence VUV spectrograph [5] indicates that the molybdenum radiation accounts for about 30% of the radiated

power from the main plasma and that the contributions due to carbon and oxygen are $\leq$ 5% and $\leq$ 10% respectively. This code assumes a circular geometry which may not properly account for the elongated plasmas and divertor of Alcator C-Mod. The uncertainties in the atomic physics relating impurity densities to radiated power, the uncertainties in determining the radiated power from the main plasma, and the neutral particle contribution may explain this discrepancy in radiated power fractions.

4. Divertor plasma measurements

The shaped divertor of Alcator C-Mod is not instrumented with enough bolometers to unambiguously obtain local emissivities without relying on assumptions about the shape and extent of the emissivity profile. An alternate method of calculating the radiated power from the divertor is to assume that the bolometer chords of an array span the entire emitting region of the divertor. For each array, individual chord brightnesses are multiplied by their poloidal widths, integrated in the toroidal direction, and then summed to give the total radiated power in the divertor.

There is significant radiated power coming from the shaped divertor region when the ion ∇B drift direction is toward the x-point (see Figure 3). This power increases linearly with density when $\overline{n}_e \geq 0.8 \times 10^{20}$ m^{-3}. When the ion ∇B drift direction is away from the x-point, limited run-time indicates that there is no significant radiation in the divertor. The fraction of the input power radiated in the shaped divertor region is nearly independent of density and is in the range $0.4 \leq P_{rad,divertor} / P_{Ohmic} \leq 0.6$. Of the power available to the scrape-off layer, $P_{SOL} = P_{Ohmic}$ -

$P_{rad,main}$, the majority (60 - 80%) of it is radiated in the divertor region (see Figure 3), indicating that the divertor is operating in the radiative divertor regime.

Vertically-viewing filtered diode arrays [6] have been used to view the plasma emission from the CIII multiplet around 4650 Å and from D_α. Together with the horizontally-viewing bolometers these measurements determine the location of the impurity radiation in the divertor. The carbon emission is strongest from the region near the outer divertor tiles and the D_α emission is most intense in the region near the inner divertor tiles. Spectroscopic measurements indicate that the molybdenum source rate and radiation from the divertor region are negligible under normal operating conditions.

There are also filtered diode arrays that view the plasma in the horizontal direction. Inversions of the approximately 200 brightness chords can be performed using the D_α or CIII data to give local emissivities [7]. The calculation of total hydrogen radiation is based on the D_α signals and Johnson - Hinnov formalism [8]. Determination of the total carbon radiation is less straightforward. Estimates of the local carbon emissivity are based on measured CIII emissivity, calculated charge-exchange profiles, and MIST modelling. Charge exchange volumetric losses have been calculated using a simple Monte Carlo code [9]. These calculations indicate that the charge-exchange neutrals are comparable to carbon radiation as contributors to the energy loss in the divertor. The deuterium radiation contribution is negligible. There is rough agreement between these local emissivities and the emissivities calculated from the divertor bolometer chord brightness data.

When divertor detachment occurs, the power flow to the divertor plates in the region near the strike points is suddenly extinguished [9]. Signatures of this detachment are: the fraction of the input power radiated from the main plasma and divertor increases and the radiation in the divertor region is rearranged spatially. The spatial rearrangement of the radiation in the divertor is illustrated by the bolometer chordal views presented in Figure 4. Divertor detachment occurs just after 0.8 sec for the discharge depicted in Figure 4. In general, it is found that for the bolometer arrays, chord B1, which is viewing well above the x-point, has an increase in brightness and all other chords have a decrease. All of the chords of the XUV array show an abrupt decrease at divertor detachment. For the particular discharge shown in Figure 4, chord B2 increases at detachment and then later decreases as the radiation moves further inside the separatrix. Overall these bolometers, together with the visible diagnostic arrays, indicate that the carbon radiation has coalesced into two regions: one near the outer divertor plate and one above the divertor but inside the last closed flux surface. The D_α radiation has also moved inside the last closed flux surface but is closer to the x-point than the carbon radiation.

5. Power balance

The power balance equation is $P_{Ohmic} = P_{rad,main} + P_{rad,divertor} + Q_{divertor}$, with the latter not directly measured at the present time. There are thermocouples embedded in the divertor plates and the bulk temperature rise of the molybdenum tiles on the plates after a high Ohmic

power discharge can be used to set an upper limit to the heat flux to the divertor. For a few such discharges (P_{Ohmic} ~ 1.4 MW) it is estimated that the heat flux to the divertor plates is ≤ 40% of the input power, while the radiated power from the main plasma is ~ 30% of the input power, and the radiated power from the divertor is ~ 45%.

Divertor detachment gives rise to a unique opportunity to check the power balance of the plasma. The reduction of the power flowing to the divertor plates, $Q_{divertor} \approx 0$, means that the power balance equation becomes $P_{Ohmic} \approx P_{rad,main} + P_{rad,divertor}$. Figure 5 illustrates this phenomenon. When the plasma detaches from the divertor plates ≥ 85% of the input power is accounted for by radiation from the main and divertor plasmas in contrast to only ≥ 60% for an attached plasma.

6. Conclusions

During Alcator C-Mod's initial operational period it was determined that typically 30 - 40% of the input power is radiated from the main plasma and 40% of the input power is radiated from the divertor region. These fractions are almost independent of density while the radiated power from these regions is linearly dependent on density. Highly radiative divertor conditions (~ 80% of the power in the SOL is radiated) have been achieved. Spectroscopic identification of impurities shows that while molybdenum is not very abundant in the main plasma it is the dominant radiation loss channel. Molybdenum source rates in the divertor region are typically too low to measure and the radiation in the divertor can be accounted for by charge exchange neutrals and deuterium, carbon, and oxygen radiation. Power balance accounting has been performed and

there is relatively good agreement between the input power and the measured power leaving the plasma. When divertor detachment occurs, the radiation in the main plasma and divertor increases. Also, the spatial location of the radiation in the divertor is rearranged with some emission from D_α and CIII coming from inside the last closed flux surface.

Acknowledgements

A special thanks to Brian LaBombard for creating the Alcator C-Mod EDGE Database. This work is supported by U.S. DoE Contract # DE-AC02-78ET51013

References

[1] I.H. Hutchinson and the Alcator Group, Physics of Plasmas, **1**, 1511 (1994).

[2] E.R. Müller, G. Weber, F. Mast, G. Schramm, E. Buchelt, and C. Andelfinger, Design of a Four-channel Bolometer Module for ASDEX Upgrade and Tore Supra, Max-Planck-Institut für Plasmaphysik IPP Report 1/224 (1985).

[3] R.A. Hulse, Nuclear Technology/Fusion, **3**, 259 (1983).

[4] M.J. May, A.P. Zwicker, H.W. Moos, M. Finkenthal, and J.L. Terry, Review of Scientific Instruments, **63**, 5176 (1992).

[5] M.A. Graf, J.E. Rice, J.L. Terry, E.S. Marmar, J.A. Goetz, G.M. McCracken, F. Bombarda, and M.J. May, submitted to Review of Scientific Instruments, (1994).

[6] J.L. Terry, J.A. Snipes, and C. Kurz, submitted to Review of Scientific Instruments, (1994).

[7] C. Kurz, J.A. Snipes, J.L. Terry, B. LaBombard, B. Lipschultz, and G.M. McCracken, submitted to Review of Scientific Instruments, (1994).

[8] L.C. Johnson and E. Hinnov, J Quant Spect Radiat Transf, **13**, 333 (1973).

[9] B. Lipschultz, G.M. McCracken, J.A. Goetz, B. LaBombard, J.L. Terry, J. Snipes, A. Niemczewski, and R. Nachtrieb, these Proceedings (PSI-11).

Figure Captions

1. Schematic of the Alcator C-Mod closed shaped divertor showing the viewing chords of the bolometer systems. Chords labeled B1 - B8 are collimated bolometers and chords labeled UV1 - UV16 are collimated photodiode detectors.

2. Scaling of the radiated power from the main plasma (squares) and the fraction of the Ohmic power radiated in the main plasma (circles) with line-averaged density for standard discharges.

3. Scaling of the radiated power from the divertor region (squares) and the fraction of the power in the scrape-off layer radiated in the divertor (circles) with line-averaged density for standard discharges.

4. Spatial rearrangement of the radiation in the divertor during detachment of the divertor. The detachment occurs at 0.805 sec. The slow time response of chords B1, B2, and B5 arises from the digital filtering used to process the bolometer data. See Figure 1 for the location of the chords shown in this Figure.

5. Scaling of the fraction of the Ohmic power radiated from the main plasma plus the divertor with line-averaged density for standard discharges (squares) and for discharges with a detached divertor (circles).

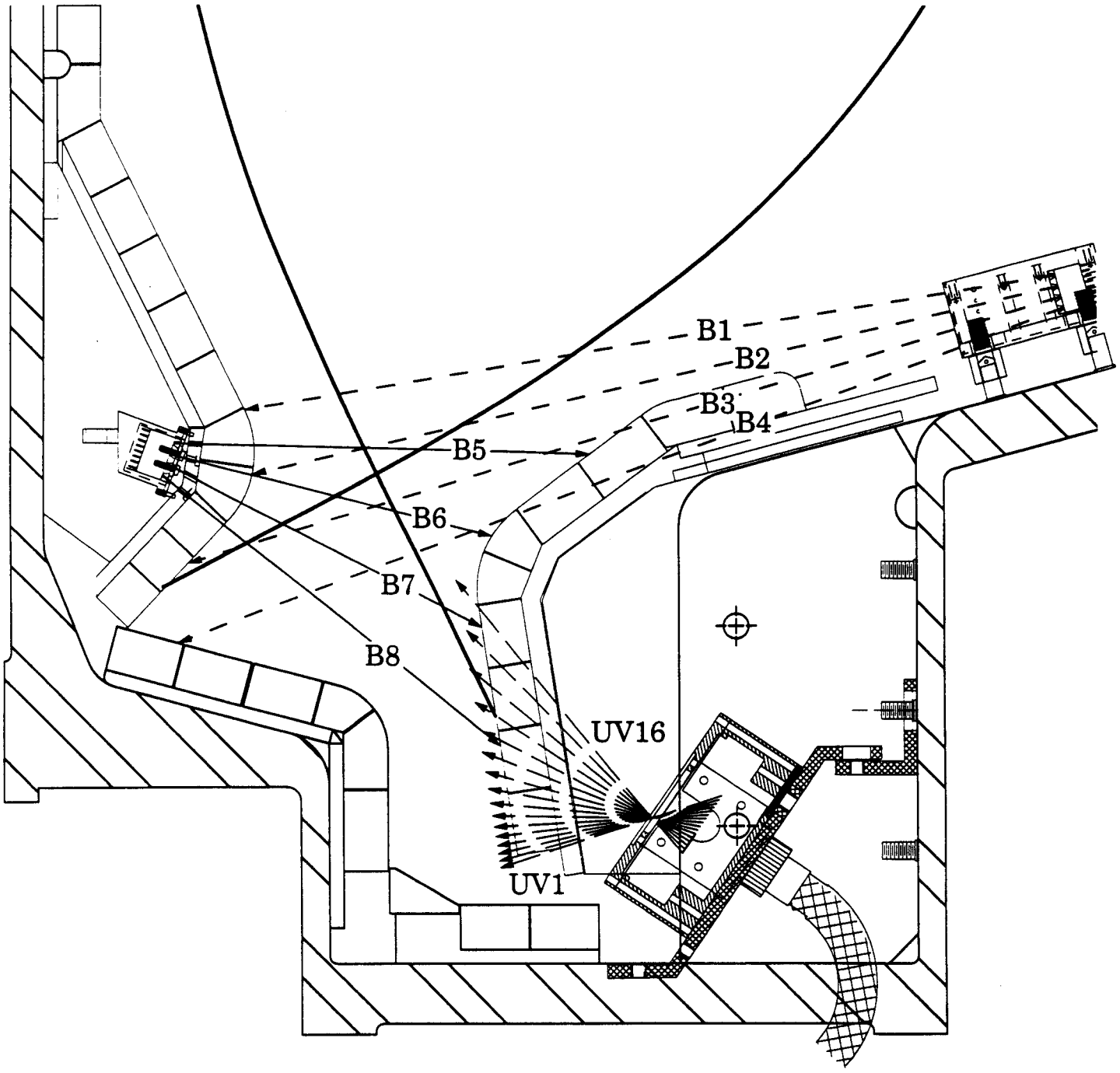

Figure 1

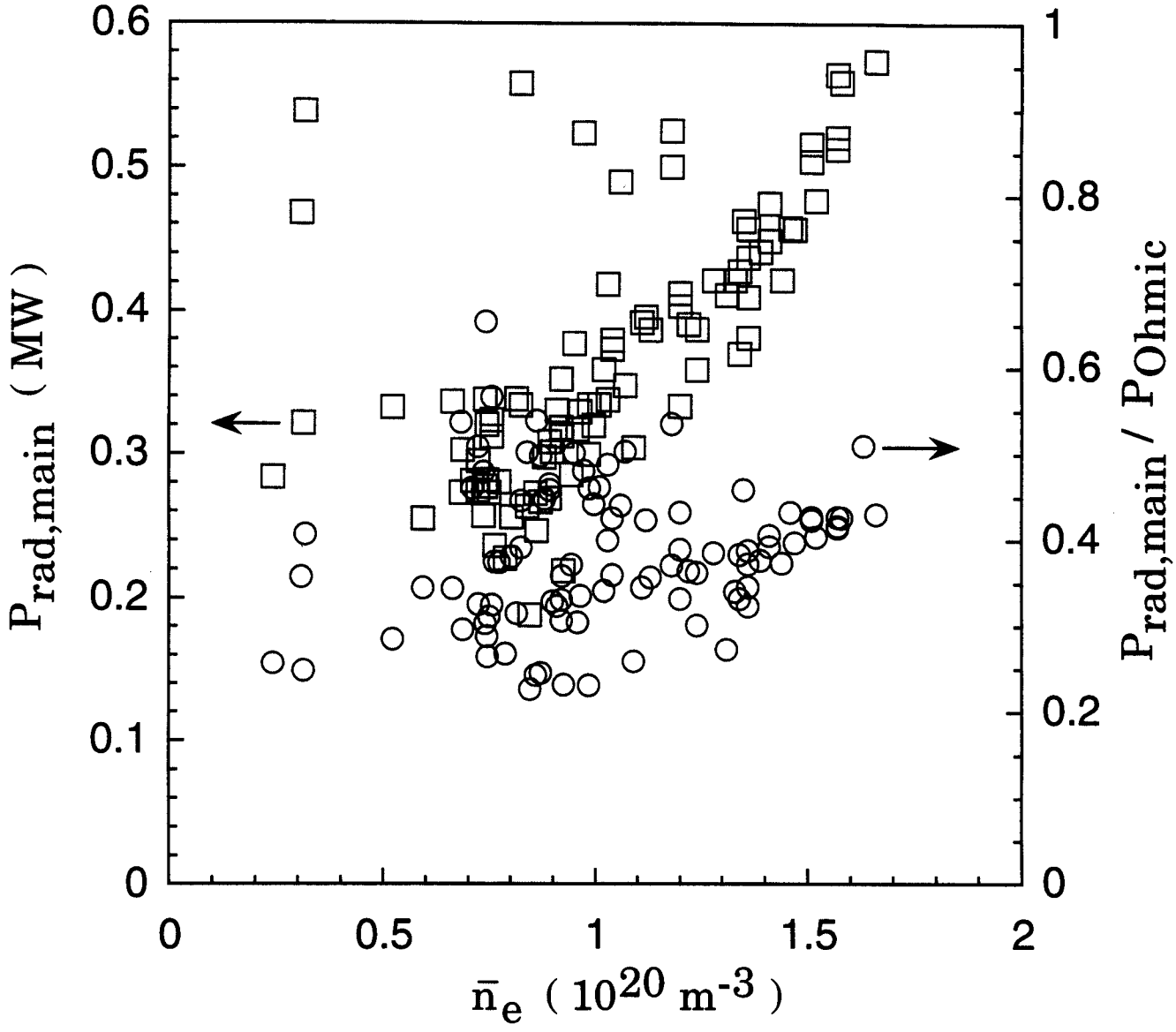
0.6
0.5
0.4
0.3
0.2
0.1
0
1
0.8
0.6
0.4
0.2
0
0
0.5
1
1.5
2
$P_{rad,main}$ (MW)
$P_{rad,main}$ / P_{Ohmic}
$\bar{n}_e$ (10^{20} m^{-3})

Figure 2

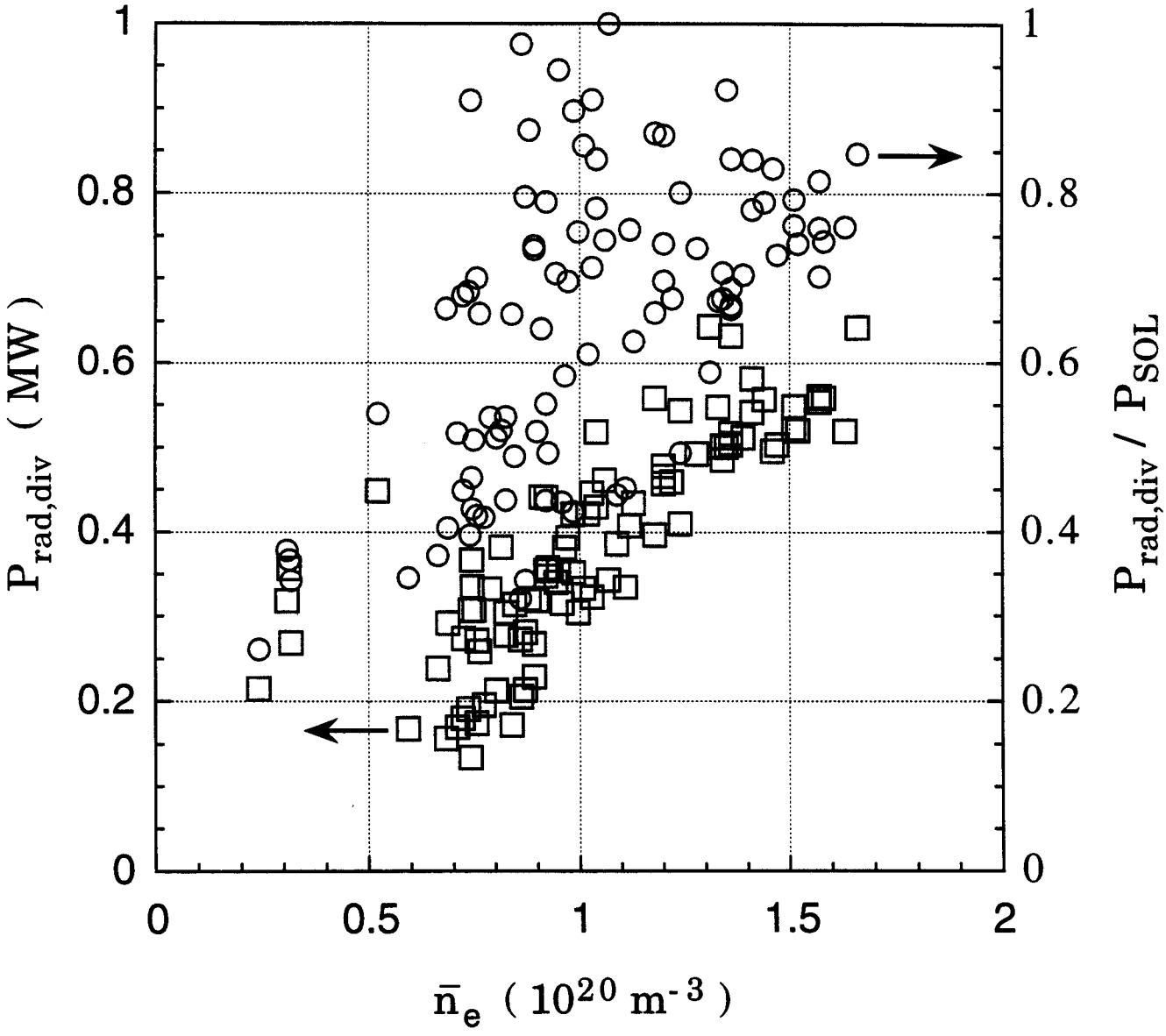

Figure 3

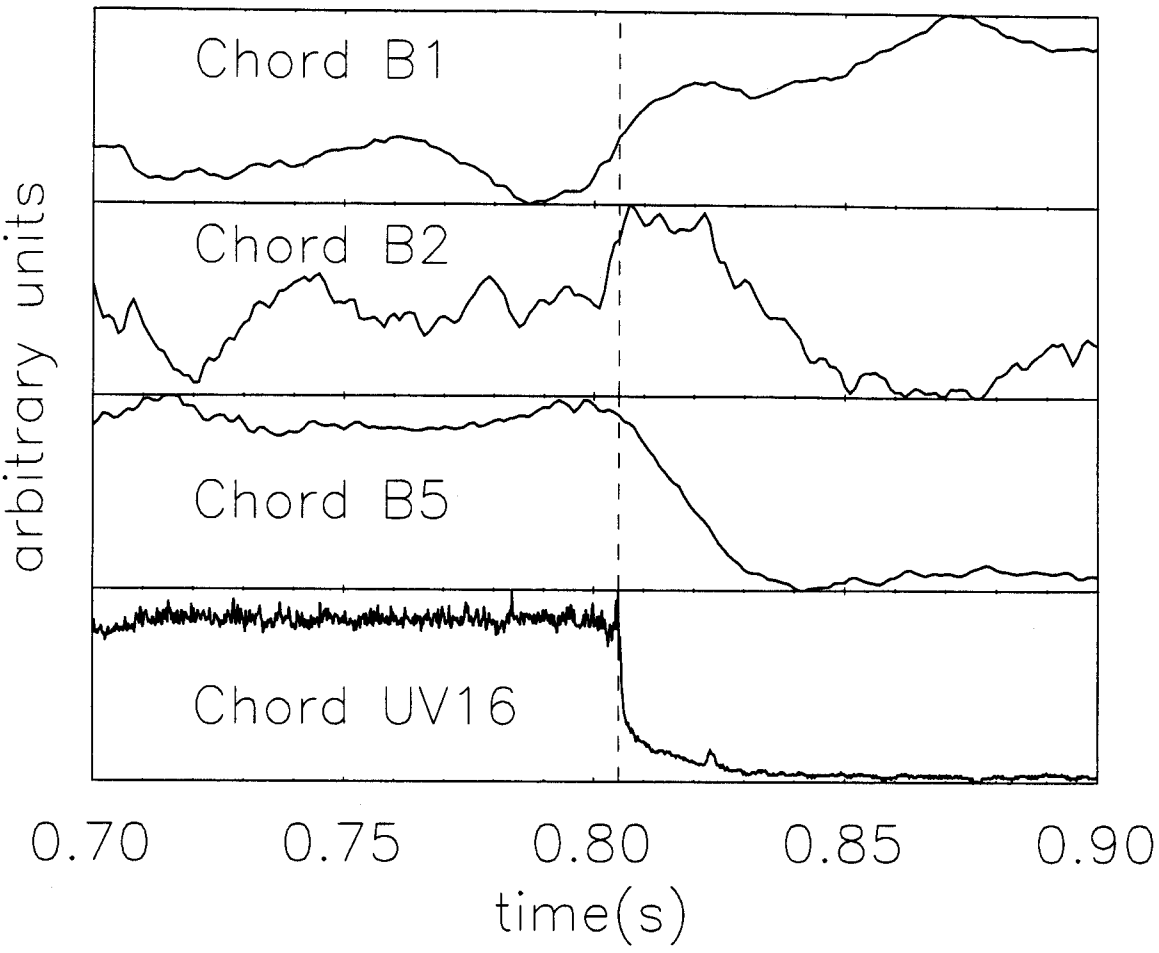
Chord B1
Chord B2
Chord B5
Chord UV16
arbitrary units
0.70
0.75
0.80
0.85
0.90
time(s)

Figure 4

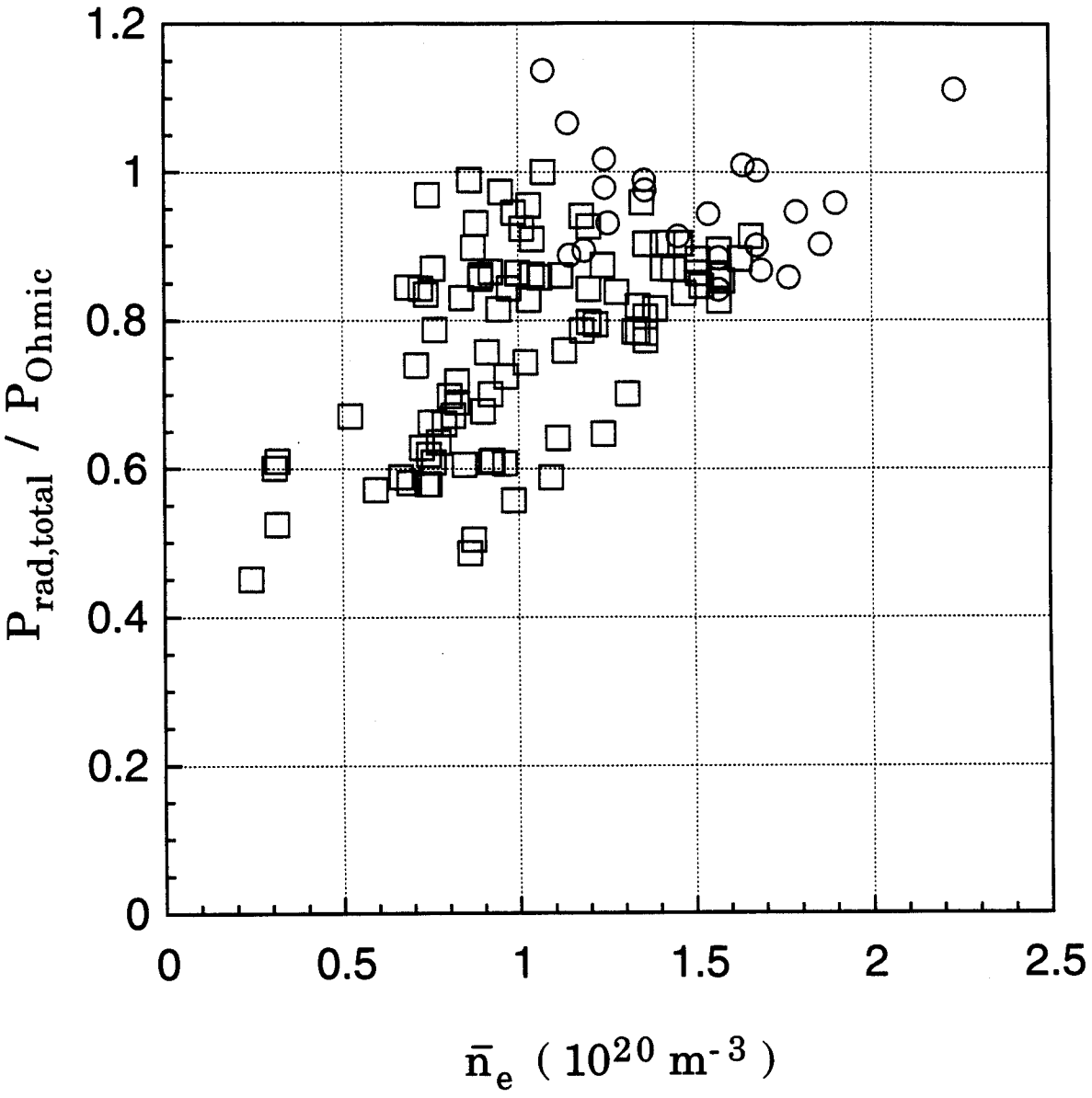

Figure 5